

A Comparative Study of Various Image Dehazing Techniques

Mohammed Mahmood Ali

Assistant Prof., Dept. of CSE,

MJCET, Hyderabad, Telangana,

mahmoodedu@gmail.com

Md. Ateeq Ur rahman

Professor, Dept. of CSE,

SCET, Hyderabad, Telangana,

mail_to_ateeq@yahoo.com

Shaikha Hajera

M.Tech. Student, Dept. of CSE,

MJCET, Hyderabad, Telangana,

shaiky696@gmail.com

Abstract: - Most of corrupted images due to various degradations involve filtration process, to efficiently make use of image scenes in image processing. Particularly, the outdoor image scenes are degraded due to cloudy medium in the atmosphere (i.e., impurities in air). Such as Hazeiness, mist, and smog are the phenomena of atmospheric absorption that scatter the image scenes. Moreover, many computer vision applications, works on input images, fail to work efficiently because of degraded images. Removing those deficiencies with the use of image haze removal techniques will assist in image comprehension and computer applications (aerial imagery or image classification). This paper surveys the existing de-hazing techniques that aid in filtering the haze from captured images and later replace with the improvised hazy free image(s).

Keywords: -Image scenes, Image haze removal, vision appln.,.

I. INTRODUCTION

Haze in atmosphere is an observable fact that obscures the cleanliness of the sky. Much of the impurities in air ranges below 1000m. Atmospheric impurities are mist, fog, and smog. Hazeiness is caused due to impurities in air. This occurs in many populated areas like industrial areas. Due to haze clarity of images will be degraded. Hazeiness constitutes of “Airlight” and “Direct attenuation” i.e., Haze = Attenuation + Airlight. While, capturing these outdoor images from poor atmospheric constraints the radiance captured by the camera from image scene is reduced in virulence along the line of sight. This arriving light is mixed with the light coming from all other directions called the Airlight. This appends whiteness inside the image, and the second component i.e., attenuation impacts in gradual loss of intensity [16]. Due to this, there exists an important decay in the color which is depicted in Figure 3. The amount of dissipating relies on the separation among the scene points and the camera. Hence, degrading is extremely variable.

Thus, images taken in bad climate (e.g., foggy or hazy) usually loose the contrast and fidelity that occurs due to the consumption of light which is scattered by the turbid medium, for example, particles and water beads in the air, during the process of propagation [1]. Apart from that, many automated systems mostly relied on the definition of the input images, fails to work efficiently due to degradation of images. Therefore, by improving this method of image haze removal process will benefit in most of image understanding and other applications (spatial imagery, image classification, image/video retrieval, remote sensing and video analysis and recognition).

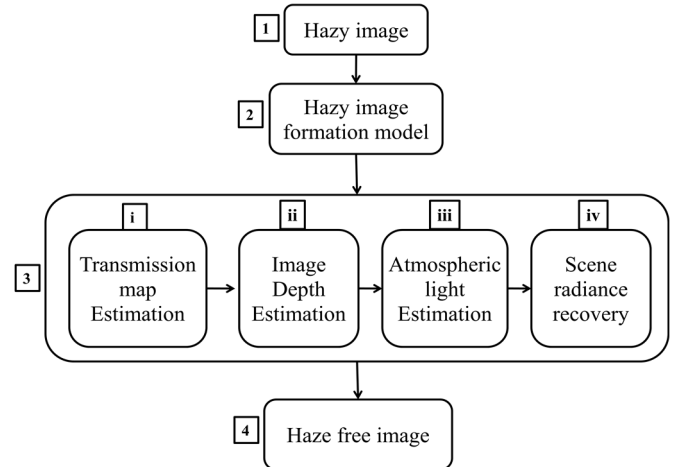


Figure.1: Block diagram of Image Dehazing

During the haze removal process the sequence of steps involved for dehazing the images are illustrated in Figure 1. The *First* step is input of haziness image. In the *Second* step whether scattering model (hazy image formation model) that performs parameters extraction from hazy images discussed in section II. Subsequently, *Third* step which is most important one in haze removal process, that has four major components (Transmission map estimation, Image depth Estimation, Atmospheric light Estimation and Scene radiance recovery) which depicts few of the methods which are used for dehazing of images is discussed in section III. *Fourth block* shows the restored image after dehazing.

Haze removal (or Dehazing) is also very much liked by consumer photography and system vision applications. Firstly, eliminating haze will drastically effects the perceptibility of the image scene and improves color shift which is affected due to airlight. Usually, the haze-free image is likely and visually attractive. Second, many of system vision algorithms, from low-level image analysis till high-level object recognition, generally presume that the input image (after radiometric calibration) has scene radiance [9].

While, heavy hazeiness in images varies from one place to other place and it is hard to predict in a hazy image. Thus, image dehazing is a difficult task. This paper describes several strategies for improving hazy images that are shot either in foggy weather conditions or other disturbances that occur in the air which destroys the cleanliness of an image and provides a comparison among the dehazing methods.

The rest of paper is structured as follows: In Section II, we reviewed the whether scattering model which is mostly used in

dehazing of images, and give a concise analysis on the parameters of this model. The Section III elaborates the various techniques used for dehazing in images. In section IV, we discussed comparison among those methods. The Section V, summarizes various techniques used for dehazing the haziness in images and suggested the better strategy to improve image scenes by removing the haziness from images.

II. MODEL FOR FORMING HAZY IMAGES

To understand the formation of hazy images, the atmospheric scattering model, which is proposed by McCartney in 1976 [18], is mostly used in Image applications. Later, Narasimhan and Nayar had further improvised the scattering model [19], [20], [22], [23].

The model is shown using Equations (1) and (2):

$$I(x) = J(x)t(x) + A(1 - t(x)) \quad \dots \dots \dots \text{Equ.(1)}$$

In which, x is the point of the pixel in the image, \mathbf{I} is the misty image, \mathbf{J} is the scene radiance that shows hazy free image, \mathbf{A} is the airlight in atmosphere, t acts as the medium transmission, β is the scattering coefficient in the air and d is the depthness of scene. \mathbf{I} , \mathbf{J} and \mathbf{A} are all three-dimensional vectors in RGB space. Since \mathbf{I} is understood, as the aim of dehazing for estimates \mathbf{A} and t , then restore \mathbf{J} as shown in Equation (1). In the equation first term, $\mathbf{J}(x)\mathbf{t}(x)$ is called the direct attenuation; the second term, $\mathbf{A}(\mathbf{1}-\mathbf{t}(x))$ is called Airlight. This haze model is directly extended to each RGB component of a color image.

It is interesting to note the depth of image scene d is most important information. Though, the scattering coefficient β is a constant in standardized atmospheric condition, the medium transmission t is easily estimated as per the Equation (2) if the deepness of image scene is given. However, the range of $d(x)$ is $(0, +\infty)$ as the scenery objects that appear in the image scene is far from the observer as discussed in Equation 3.

Equation (3) shows that the intensity of the pixel, which makes the depth tend to infinity, can stand for the value of the atmospheric light \mathbf{A} .

The Section III, illustrates the survey of different methods used in image dehazing.

III. DIFFERENT DEHAZING METHODS

In the adverse weather conditions the atmosphere contains the haze. This significantly reduces the color and contrast of the images. For the haze removal different methods is illustrated in Figure 2.

A. Polarization Filter

In [3] paper, Yoav Y. Schechner suggested that usually airlight is scattered by the impurities in air is partly

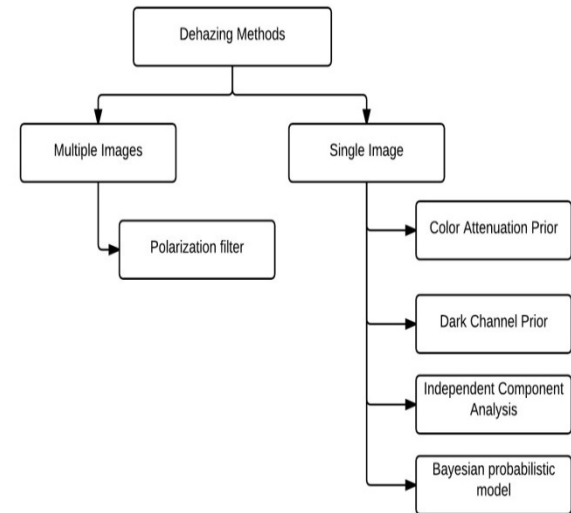


Fig.2: Different Dehazing Methods.

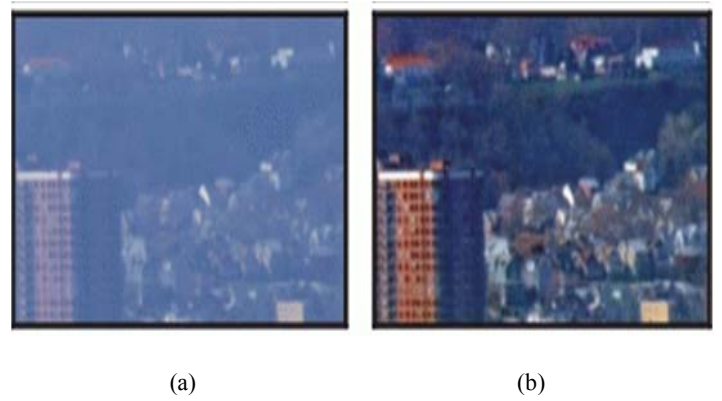


Fig.3: Result of using polarization filter method (a) Hazy image, (b) Dehazed image.

polarized. Only, polarization filters alone couldn't eliminate the haziness as illustrated in Figure 3. In his paper authors elaborates the image creation process through the polarization effect of the whether scattering and inverting it, for getting a hazy free image.

In this method multiple input images has similar scene that has been captured from various bad weather conditions. Usually, the image constitutes of the two not known components, first one is the image scene radiance in the absence of the haziness and the other one is airlight. To replace those two not known components two independent images are required. Usually the airlight, is partially polarized. This paper also describes an approach that does not require the weather conditions to improve and it can be applied instantly. Those image scenes taken from polarizer uses polarization filtering technique.

The polarization filtering and the orientation of the polarization filter improved the contrast of the single input image. In order to resolve this issue of haziness, polarization filtering is used to determine the haze content of image and then this haze contents are eliminated from the image to get the clear image is depicted in Figure 3.



(a)

(b)



(c)

(d)

Fig.4: Color attenuation results of prior method (a) Hazy image, (b) Restored depth map, (c) Restored transmission map (d) Dehazed image.

B. Color Attenuation Prior

Qingsong Zhu had presented a naive color attenuation prior method, which is benefitted to recover the depth information from any one of hazy image directly [9]. This easy and strong prior aids to create a linear model for the image scene depth of the hazy images. By learning these parameters of the linear model with a supervised learning technique, the bridge between the hazy images and its consequent depth map is built efficiently. With the use of recovered depth information technique, the haze from a single hazy image is removed. An overview of proposed dehazing technique is depicted in Figure 4. The efficiency in dehazing method is extremely increased and the dehazing efficiency is better instead of prevailing dehazing algorithms.

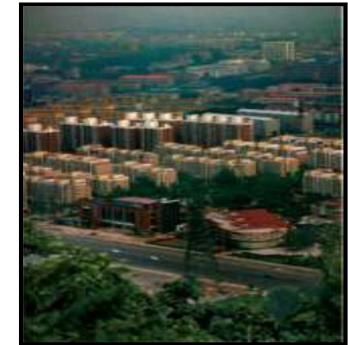
C. Prior Dark Channel

Kaiming He *et. al.*, developed a naive prior—prior dark channel—for an image haze removal [2]. The prior dark channel depends on the Number of occurrences of outdoor hazy free images. They found that, in many of image regions could not be captured from the sky, few pixels (well-known as dark pixels) had less intensity in utmost one color (RGB) channel. In hazy images, the intensity of those dark pixels in specific channel is due to the airlight. Therefore, those dark



(a)

(b)



(c)

Fig.5: Result of dark channel prior method (a) Hazy image, (b) Restored depth map, (c) Dehazed image.

pixels assist in accurate estimation for haze transmission. Combining a haze imaging model and a soft matting interpolation method recovered a high-quality haze free image and produced a good depth map.

This strategy is valid that can handle long objects in heavily hazy images. They do not rely on significant variance of transmission or surface shading. The results obtained had few halo artifacts. Like any approach using a strong assumption, his approach also has its own limitation. The prior dark channel will be invalid in the scenario where the scene object is intrinsically alike to airlight (e.g., snowy ground-level or a whitish wall) over a big resident region and without shadow is cast on it. Although the approach works well for most outdoor hazy images, it may fail on some extreme cases.

D. Independent Component Analysis

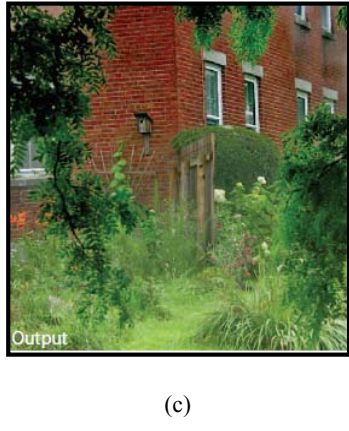
Raanan Fattal, also presented an approach that recovers a haze-free image given as input i.e., photograph. He achieved this by interpreting the image through a developed model that considers only surface shading apart from image scene transmission. Based on such refined image formation model, the image scene is classified as local regions of a constant albedo and the airlight-albedo ambiguity is solved through deriving an extra condition that needs the surface shading apart from scene transmission functions to be locally statistically uncorrelated.



(a)

(b)

Depth



(c)

Fig.6: Result of Independent Component analysis method (a) Hazy image, (b) Restored depth map, (c) Dehazed image.

This needs the coloring component to vary significantly compared to the impurities exists within the image. He used a graphical model to propagate the solution to pixels in which the signal-to-noise ratio falls below an admissible level that is derived analytically. Subsequently, airlight color is also predicted with the use of un-correlation principle. This strategy is *passive*; it do not require many image scenes, any light-blocking based polarization, any form of scene depth information, or any specialized sensors or hardware.

The strategy adopts less requirement of a *single* image learned by normal consumer camera. It also, don't picks the haze layer to be flat in space, i.e., discontinuities in the image scene depth as permitted.

As depicted in Figure 6, inspite of these challenges this problem poses, this strategy gains a significant decrease in airlight and replaces the contrasts of complex scenes. But, this strategy takes much time and hence, is not used for grayscale image scene dehazing. Furthermore, it had few issues to handle with dense-haze images.

E. Bayesian Probabilistic Model

Nishino *et. al.*, employed a Bayesian model [6]. Whether conditions are influenced by deferred particles, such as mist and haze that severely modify the image scenes. Replacing of such image scene from the single observation made in such bad weather conditions becomes bit difficult due to haziness



(a)

(b)

Fig.7: Result of Bayesian probabilistic method (a) Hazy image, (b) Dehazed image.

that arises inside the image. In his paper, they used Bayesian probabilistic model for estimating the image scene albedo and depth for the misty scenes by leveraging of latent statistics.

Their key approach is to develop the image with a factorial Markov random field (FMRF) in which the scene albedo and depth are two relatively independent hidden layers that aids to jointly estimate them. They also, derived the joint estimation technique which is based on Bayesian formulae for factorizing the foggy images into its image scene albedo and depth, through exploiting existing image and depth statistics as done prior on those latent layers that aids in estimating of scene albedo and depth along with canonical expectation maximization algorithm and resolved bilinear ambiguity as depicted in Figure 7.

IV. QUALITATIVE AND QUANTITATIVE COMPARISON

In order to compare the efficiency of the dehazing method, a test is performed on various misty images and compared with He *et.al*'s., [2], Fattalet *et.al*'s [1], Nishino *et.al*'s [6], and Q. Zhu *et.al*'s [9] methods.

As all the dehazing strategies could get really fine outputs by dehazing the general outdoor images, it is difficult to rank them visually [9]. In order to judge against them, a survey is carried on various algorithms on some challenging images with large whitish or gray regions, since most existing dehazing algorithms are not responsive to the white color.

Figure 8, depicts the qualitative comparison of outputs with the existing dehazing technique on challenging real-world images. Figure 8(a) depicts the images seems to be dehazed. Figure 8(b-e) shows the outputs of Tarel *et al.*, Nishino *et al.*, He *et. al.*, and Zhu *et al.*, respectively. It is depicted in Figure 8(b), much of the haziness is filtered in Tarel's outputs, and the details of the scenes and objects are well replaced. However, the results significantly suffer from over-enhancement (for example, the sky region of the initial image is much darker than it has to be).The reason is Tarel's method is similar to He *et. al.*, strategy that has an inherent problem of over estimating the transmission as discussed.

Furthermore, halo artifacts seems to have discontinuities in Figure 8(b) (see the mountain in the initial image and the leaves of plant in the next image) due to that the "median

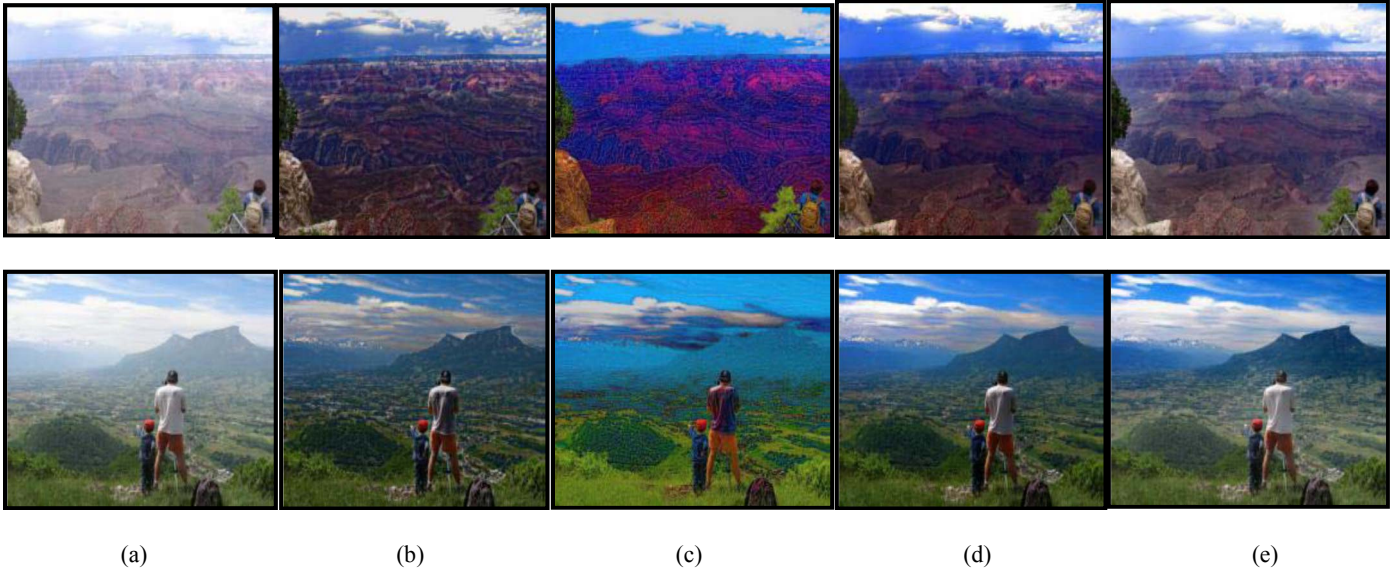


Fig.8: Qualitative comparison of different methods on real-world images. (a) The hazy images. (b) Tarel et al.’s results. (c) Nishino et al.’s results. (d) He et al.’s results. (e) Zhu’s results.

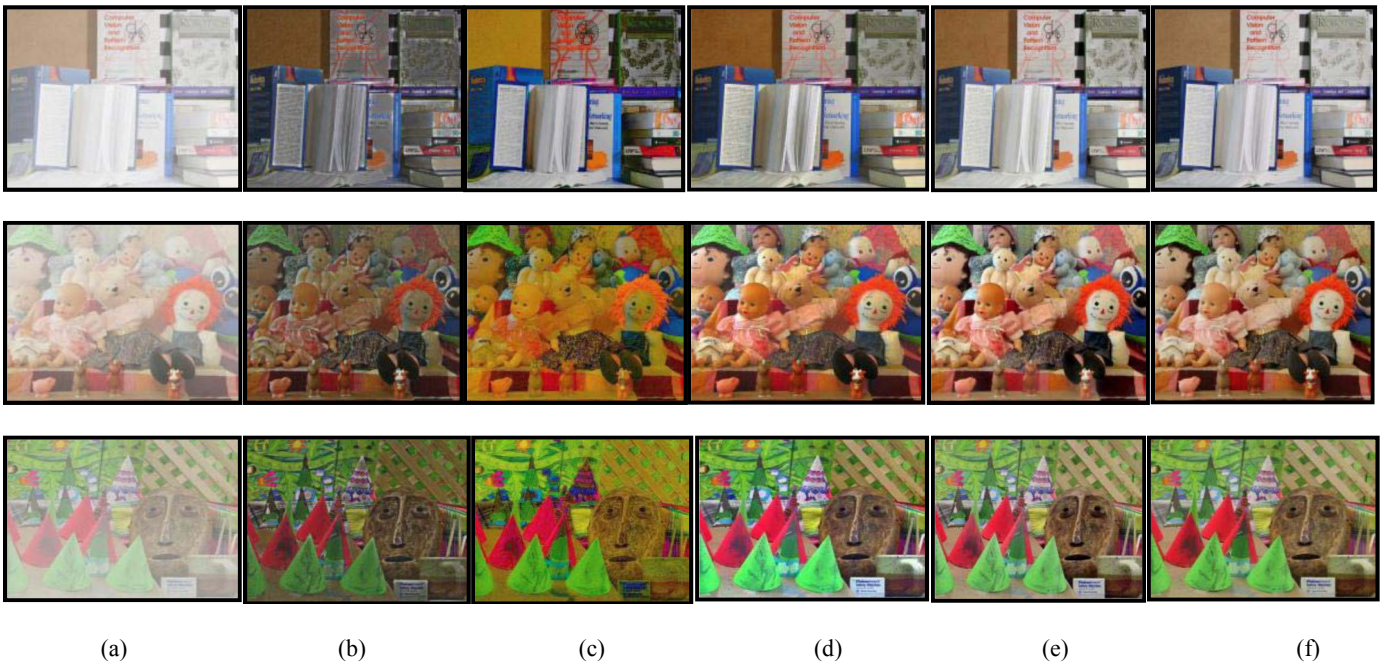


Fig.9: Qualitative comparison of different methods on Synthetic images. (a) The haziness image scenes. (b) Tarel et. al.’s, outputs. (c) Nishino et. al.’s, outputs. (d) He et. al.’s, outputs. (e) Q Zhu et. al.’s, outputs. (f) Ground truth

filter” is used, which is not an edge-preserving filter [4]. The outputs of Nishino *et. al.*, have a similar difficulty as Nishino *et. al.*, strategy, seems to enhance the inner contrast of the image scene. As seen in Figure 8(c), the restored images are oversaturated and distorted, particularly in the next image (the color shade of the shirt is changed to dark). In contrast, the outputs of He *et. al.*, are much enhanced visually (see Figure 8(d)). The dense mist distance is removed, and there are no halo artifacts.

Nevertheless, color distortion still appears in the regions with white objects as observed in third image of shirt. The reason can be explained as follows: As the method of recovering the transmission is used [2], which is totally depends on the prior dark channel, the accuracy of the estimation strongly based on the expiry of the prior dark

channel. Unluckily, this prior is unacceptable in scenarios where the scene brightness is alike to the airlight, and the estimated transmission is thus not reliable enough in some cases. In adding up, the weather light is also a significant factor for calculating the transmission. Therefore, obtaining the correct transmission, a precise estimation from whether airlight is one of necessary constraint. However, the approach for estimating the airlight proposed by He *et. al.*, has its restriction and the estimated result is fairly accurate. For this reason, He *et. al.’s*, approach is prone to overestimating the transmission. Compared with the outputs of the three methods, the outputs of Qingsong Zhu are free from oversaturation. As displayed in Figure 8(e), the sky and the cloud in the images are lucid and the details of the mountains are improved fairly.

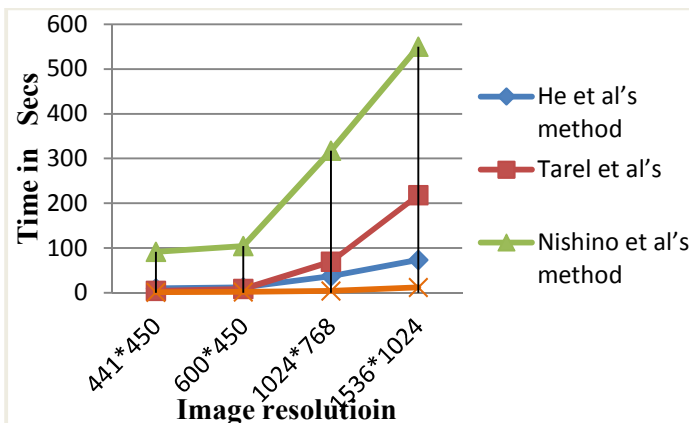


Fig.9: Time Consumption Comparison among He et al. [2], Tarel et al. [4], Nishino et al. [5], and Q zhu et al. [9].

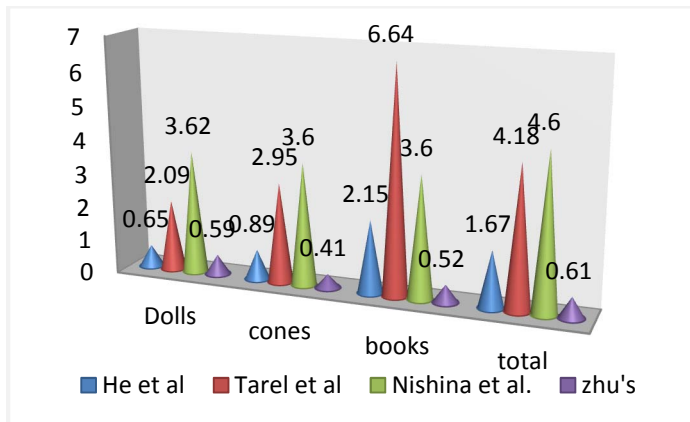


Fig.10: MSE of different methods.

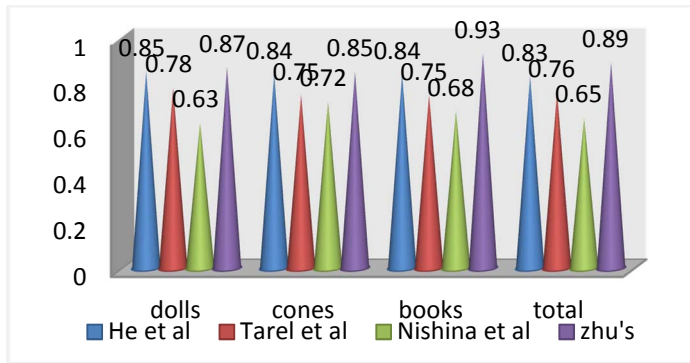


Fig.11: SSIM of different methods.

Table.1: Five indicators calculated on the image of figure 8.

Mountain			
Methods	Tarel et al.'s [4]	He et al.'s [2]	Zhu et al.'s [9]
e	0.4753	0.1301	0.1023
r	1.5621	1.1821	1.1511
CCI	46.5472	42.8	43.12
CNI	0.7003	0.93	0.7531
CNC	2.373	2.731	2.425

To quantitatively assess and compare the methods, the mean squares error (MSE) and the structural-similarity (SSIM) measures are taken for the images which is depicted in Figure 9. The MSE of each image result can be calculated by the following equation(4).

$$e = \sqrt{\frac{1}{3N} \sum_{c \in \{r,g,b\}} \|J^c - G^c\|^2} \quad \dots \text{Eqn.(4)}$$

where \mathbf{G} is the ground truth image, \mathbf{J} is the dehazed image, J^c represents a color channel of \mathbf{J} , N is the number of pixels in the image \mathbf{G} , G^c represents a color channel of \mathbf{G} , and e is the MSE measuring the achievement between dehazed image \mathbf{J} and the ground truth image \mathbf{G} . Given \mathbf{J} and \mathbf{G} , a low MSE represents the dehazed result is satisfying while a high MSE means that the dehazing effect is not satisfactory.

Additionally in Figure 10 the MSEs outputs obtained by different algorithms. As discussed in Nishino et. al.'s., is highest MSEs. The elevated MSEs are primarily because of the over-enhancements mentioned earlier. Tarel et al.'s, results do better than Nishino et al.'s., in the last two images while they perform poorer in the books images. The total MSE of He et al.'s., results is 0.0167, which is more than double than the other. In contrast, Q zhu et al.'s., method achieves the lowest MSEs in all cases.

The structural similarity (SSIM) image quality assessment index [24] is introduced to assess the ability to preserve the structural information of the algorithms. A high SSIM represents high similarity between the dehazed image and the ground truth image, while a low SSIM conveys the contradictory meaning. Figure 11, depicts the SSIMs of outputs in Figure 9. The SSIMs of Nishona et. al.'s., outputs are all lower than 0.7 indicating that much structural information in the images has been lost. It is clear that the SSIMs of He et.al., are much higher than the other in the images. Q zhu e.t al's., results attain the highest SSIMs outperforming the three algorithms.

The two types of no-reference objective estimation criteria are also used for quantitative comparison which is based on visible edges and image color provided by Guo et al. [25], Hautire et al., [26] & Huang et al., [27]. They used assessment methods which mainly include five indicators: the average gradient ratio after and before restoration r , the ratio of new visible edges e color naturalness index CNI , contrast naturalness colorfulness CNC , and color colorfulness index CCI . r and e primarily assess the capability of contrast restoration, and CCI and CNI are used for evaluating naturalness and colorfulness of color images from the perspective of color saturation. The last indicator CNC is a evaluation index to assess the algorithm performance comprehensively. Usually, higher the values of these indicators are, then better the dehazing approach performs. Table 1, show quantitative values computed on the top row results in Fig. 8.

V. DISCUSSION & CONCLUSION

In this paper, we have presented various methods that are helpful in image dehazing. An hazy image is distinguished with an important attenuation of color which particularly depends proportionally with the distance to the

scene objects. Due to which, the existing natural contrast is diminished and the image characteristics steadily fades as they are far away from the camera sensor. Most of the dehazing techniques are useful in surveillance, intelligent vehicles, and remote sensing of images as well as under water imaging, etc. These methods are based on the partial estimation of whether conditions and airlight. As all the dehazing strategies are feasible to really good experimental results after dehazing of wide-range of image scenes, when compared with the results obtained of those three algorithms, the outputs of Qingsong Zhu are free from oversaturation. The comparative results are depicted in Figure 8, which shows the improvised image after removal of haziness from image scenes in Figure 8(e) where the sky and the cloud inside the image is clear and the details of the mountains are enhanced moderately.

References

- [1] R. Fattal, "Single image dehazing," *ACM Trans. Graph.*, vol. 27, no. 3, p. 72, Aug. 2008.
- [2] K. He, J. Sun, and X. Tang, "Single image haze removal using dark channel prior," *IEEE Trans. Pattern Anal. Mach. Intell.*, vol. 33, no. 12, pp. 2341–2353, Dec. 2011.
- [3] Y. Y. Schechner, S. G. Narasimhan, and S. K. Nayar, "Instant dehazing of images using polarization," in *Proc. IEEE Conf. Comput. Vis. Pattern Recognit. (CVPR)*, pp. No. 325–332, 2001.
- [4] J.-P. Tarel, N. Hautière, L. Caraffa, A. Cord, H. Halmaoui, and D. Gruyer, "Vision enhancement in homogeneous and heterogeneous fog," *IEEE Intell. Transp. Syst. Mag.*, vol. 4, no. 2, pp. 6–20, Apr. 2012.
- [5] L. Kratz and K. Nishino, "Factorizing scene albedo and depth from a single foggy image," in *Proc. IEEE 12th Int. Conf. Comput. Vis. (ICCV)*, pp. 1701–1708, 2009.
- [6] K. Nishino, L. Kratz, and S. Lombardi, "Bayesian defogging," *Int. J. Comput. Vis.*, vol. 98, no. 3, pp. 263–278, Jul. 2012.
- [7] F. Meng, Y. Wang, J. Duan, S. Xiang, and C. Pan, "Efficient image dehazing with boundary constraint and contextual regularization," in *Proc. IEEE Int. Conf. Comput. Vis. (ICCV)*, pp. 617–624, 2013.
- [8] B. Xie, F. Guo, and Z. Cai, "Improved single image dehazing using dark channel prior and multi-scale retinex," in *Proc. Int. Conf. Intell. Syst. Design Eng. Appl.*, pp. 848–851, 2010.
- [9] Q. Zhu, J. Mai, and L. Shao, "A Fast Single Image Haze Removal Algorithm Using Color Attenuation Prior," *IEEE Trans., on Image Processing*, Vol. 24, No. 11, pp. 3522–3533, 2015.
- [10] J. Kopf et al., "Deep photo: Model-based photograph enhancement and viewing," *ACM Trans. Graph.*, vol. 27, no. 5, p. 116, Dec. 2008.
- [11] S.-C. Pei and T.-Y. Lee, "Nighttime haze removal using color transfer pre-processing and dark channel prior," in *Proc. 19th IEEE Conf. Image Process. (ICIP)*, Sep./Oct. pp. 957–960, 2012.
- [12] Q. Zhu, S. Yang, P. A. Heng, and X. Li, "An adaptive and effective single image dehazing algorithm based on dark channel prior," in *Proc. IEEE Conf. Robot. Biomimetics (ROBIO)*, Dec. pp. 1796–1800, 2013.
- [13] F. Zhu and L. Shao, "Weakly-supervised cross-domain dictionary learning for visual recognition," *Int. J. Comput. Vis.*, vol. 109, nos. 1–2, pp. 42–59, Aug. 2014.
- [14] S. K. Nayar and S. G. Narasimhan, "Vision in bad weather," in *Proc. IEEE Int. Conf. Comput. Vis. (ICCV)*, vol. 2, pp. 820–827, 1999.
- [15] VinkeySahu and VinkeySahu, "A Survey Paper On Single Image Dehazing", IJRITCC Volume: 3 Issue: 2 February 2015.
- [16] Ruchika Sharma and Dr. Vinay Chopra, "A Review on Different Image Dehazing Methods" International Journal of Computer Engineering and Applications, Volume VI, Issue III, 2014.
- [17] AtulGujral, Aditi, Shailesh Gupta and Bharat Bhushan, "A Comparison Of Various Defogging Techniques", International Journal of Signal Processing, Image Processing and Pattern Recognition, Vol.7, No.3, 2014.
- [18] E. J. McCartney, Optics of the Atmosphere: Scattering by Molecules and Particles. New York, NY, USA: Wiley, 1976.
- [19] S. G. Narasimhan and S. K. Nayar, "Removing weather effects from monochrome images," in *Proc. IEEE Conf. Comput. Vis. Pattern Recognit. (CVPR)*, pp. II-186–II-193, 2001.
- [20] S. K. Nayar and S. G. Narasimhan, "Vision in bad weather," in *Proc. IEEE Int. Conf. Comput. Vis. (ICCV)*, vol. 2, Sep., pp. 820–827, 1999.
- [21] S. G. Narasimhan and S. K. Nayar, "Vision and the atmosphere," *Int. J. Comput. Vis.*, vol. 48, no. 3, pp. 233–254, Jul. 2002.
- [22] J. Kopf et al., "Deep photo: Model-based photograph enhancement and viewing," *ACM Trans. Graph.*, vol. 27, no. 5, p. 116, Dec. 2008.
- [23] S. G. Narasimhan and S. K. Nayar, "Contrast restoration of weather degraded images," *IEEE Trans. Pattern Anal. Mach. Intell.*, vol. 25, no. 6, pp. 713–724, Jun. 2003.
- [24] Z. Wang, A. C. Bovik, H. R. Sheikh, and E. P. Simoncelli, "Image quality assessment: From error visibility to structural similarity," *IEEE Trans. Image Process.*, vol. 13, no. 4, pp. 600–612, Apr. 2004.
- [25] F. Guo and Z. Cai, "Objective assessment method for the clearness effect of image defogging algorithm," *Acta Autom. Sin.*, vol. 38, no. 9, pp. 1410_1419, Sep. 2012.
- [26] N. Hautière, J.-P. Tarel, D. Aubert, and É. Dumont, "Blind contrast enhancement assessment by gradient ratioing at visible edges," *Image Anal. Stereol. J.*, vol. 27, no. 2, pp. 87_95, Jun. 2008.
- [27] K.-Q. Huang, Q. Wang, and Z.-Y. Wu, "Natural color image enhancement and evaluation algorithm based on human visual system," *Comput. Vis. Image Understand.*, Vol. 103, No. 1, pp. 52_63, 2006.